Analytica Chimica Acta 1310 (2024) 342703

Contents lists available at ScienceDirect

Analytica Chimica Acta

journal homepage: www.elsevier.com/locate/aca

A novel split PEC sensor based on magneto–optic nanostructure and photocurrent polarity switching strategy

Xiang Ren [a], Man Wang [a], Jinxiu Zhao [a,b,**], Jinhuan Zhang [a], Jingui Chen [a], Faying Li [a,c,***], Qin Wei [a,d,*], Huangxian Ju [a,e]

[a] Key Laboratory of Chemical Sensing & Analysis in Universities of Shandong, School of Chemistry and Chemical Engineering, University of Jinan, Jinan, 250022, PR China
[b] School of Materials Science and Engineering, University of Jinan, Jinan, 250022, PR China
[c] School of Chemistry and Pharmaceutical Engineering, Shandong First Medical University & Shandong Academy of Medical Sciences, Taian, 271016, PR China
[d] Department of Chemistry, Sungkyunkwan University, Suwon, 16419, Republic of Korea
[e] State Key Laboratory of Analytical Chemistry for Life Science, School of Chemistry and Chemical Engineering, Nanjing University, Nanjing 210023, PR China

HIGHLIGHTS

- Fe_3O_4@SiO_2@CdS has good magnetic properties.
- The detection limit of CEA was 0.34 pg/mL.
- The construction strategy of the sensor is polarity inversion.
- ZnO/CuO with excellent photocurrent activity was chosen as the marker.

GRAPHICAL ABSTRACT

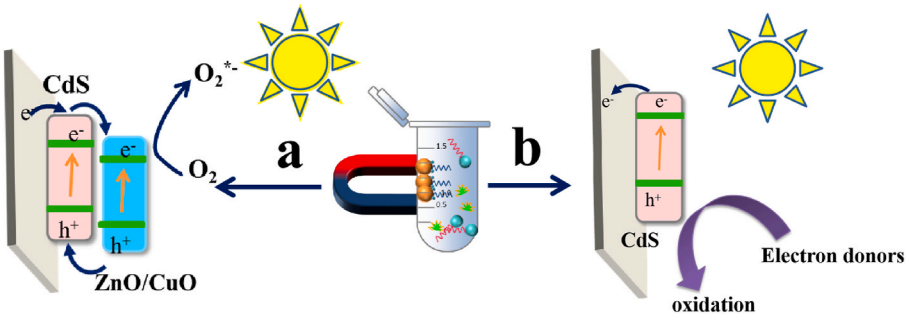

ARTICLE INFO

Handling Editor: Dr Jing-Juan Xu

Keywords:
Photoelectrochemical
Magneto–optic nanostructure
Split
Polarity conversion

ABSTRACT

Background: Photoelectrochemical (PEC) sensors have attracted much attention due to their low cost, simple instrumentation and high sensitivity. However, conventional PEC sensors require layer–by–layer modification of the photoelectrode surface, which has the disadvantages of being time–consuming and unstable. In addition, complex interfering substances in real samples may lead to false–positive or false–negative detection results. It was thought that the above drawbacks could be eliminated by the construction of a polarity inversion PEC sensor. In this work, a magnetically separated PEC sensor was constructed for the detection of Carcinoembryonic antigen (CEA).

* Corresponding author. Key Laboratory of Chemical Sensing & Analysis in Universities of Shandong, School of Chemistry and Chemical Engineering, University of Jinan, Jinan, 250022, PR China.
** Corresponding author. Key Laboratory of Chemical Sensing & Analysis in Universities of Shandong, School of Chemistry and Chemical Engineering, University of Jinan, Jinan, 250022, PR China.
*** Corresponding author. Key Laboratory of Chemical Sensing & Analysis in Universities of Shandong, School of Chemistry and Chemical Engineering, University of Jinan, Jinan, 250022, PR China.
E-mail addresses: mse_zhaojx@ujn.edu.cn (J. Zhao), lifaying89@163.com (F. Li), sdjndxwq@163.com (Q. Wei).

https://doi.org/10.1016/j.aca.2024.342703
Received 8 April 2024; Received in revised form 7 May 2024; Accepted 8 May 2024
Available online 8 May 2024

Results: During the experiment, the construction of the sensor was used for sensitive detection of CEA. In the experimental process, Fe_3O_4@SiO_2@CdS, a semiconductor material with magnetic properties, was chosen as the substrate material, and ZnO/CuO was used as the marker on the DNA_2 molecule, and a split magnetic separation PEC sensor was constructed, which was used to realize the sensitive detection of CEA. Eventually, the detection range of the sensor for CEA detection is 1–10000 pg/mL, with the detection limit of 0.34 pg/mL. Additionally, the PEC sensor has the advantages of high speed, high efficiency, high sensitivity, good specificity, and high stability. The sensing platform constructed in this work can also be extended to detect other targets, which provides a new idea for PEC sensing platforms.

Significance: In this experiment, we developed a split PEC immunosensor based on magneto–optic nanostructure and photocurrent polarity switching strategy. Specifically, the proposed magnetic nanostructure Fe_3O_4@SiO_2@CdS–DNA_1 exhibits good paramagnetism and dispersion ability. By magnetic separation process, the PEC signals of opposite polarity can be obtained.

1. Introduction

Cancer is the natural enemy of human health from beginning to end. Early detection and treatment can greatly improve the cure rate of cancer [1]. Carcinoembryonic antigen (CEA) is an acidic glycoprotein on the surface of cancer cells differentiated from endoderm cell [2]. It is considered abnormal when its concentration is greater than 5.0 ng/mL and can be detected in human serum, gastric juice, sweat and urine, and other body fluids and feces, and it is a broad–spectrum tumor marker [3]. A variety of cancers can lead to an increase in the content of CEA, such as gastric cancer, lung cancer, ovarian cancer and so on [4,5]. Therefore, the detection of CEA is of great significance in the early diagnosis and disease detection of cancers [6,7]. It is very important to find a fast and efficient detection method. Researchers have developed many modes for CEA detection, such as electrochemical detection, fluorescence detection, electrochemiluminescence detection and so on [8,9].

Compared to other means of detections, photoelectrochemical (PEC) sensor has received much attention from many researchers due to its low background signal, simple equipment, convenient operation, and low cost [10,11]. The main principle of PEC detection is to connect the change of the concentration of the detected substance with the change of photocurrent signal to realize the detection of the target [12–14]. Normally, signal on and signal off are the two main PEC signal strategies [15]. In general, signal–open PEC sensors are better than signal–closed PEC sensors because they can theoretically achieve a wider detection range, lower background signal, and less possibility of false–positive results [16]. Whereas, there are still some deficiencies in the interference of oxidizing or reducing species in complex samples. In addition, the construction of a traditional PEC sensor needs to be modified layer by layer on the surface of the photoelectrode. Therefore, the traditional model had several shortcomings, including long operation time, poor stability, and inaccurate test results caused by real sample interferences [17,18]. It is of great significance to explore a sensor platform that can overcome the above shortcomings. In recent years, with the introduction of the target, the polarity switching strategy of the photocurrent direction has been rapidly developed, which can effectively avoid false positive or false negative detection results during the detection process [19,20]. But the traditional pattern of layer–by–layer decoration is still a challenge that needs to be solved urgently. Fortunately, a recently reported PEC immunosensor based on magnetic separation technology can address this shortcoming [21,22]. The immunization process is carried out in solution, and the photocurrent of the immunoreacted product is obtained by magnetic separation [23]. Therefore, the instability and cumbersomeness of the layer–by–layer modification mode are avoided. In this work, a novel PEC immunosensor was developed based on the polarity switching strategy and magnetic separation technology.

Specifically, as a kind of superparamagnetic nanomaterial, Fe_3O_4 has excellent water dispersion ability, excellent biocompatibility, and stability, and has a broad application prospect in the field of PEC immunosensors [24]. In this study, Fe_3O_4@SiO_2@CdS nanostructures with magneto–optical properties were further synthesized using Fe_3O_4 as a matrix. The Fe_3O_4@SiO_2@CdS nanomaterials have both the superparamagnetic properties of Fe_3O_4 and the excellent photoelectric conversion ability of CdS [25]. As an n–type semiconductor with a wide band gap of 3.37 eV, ZnO owns the advantages of better stability and biocompatibility. Whereas, the large bandgap limited the light absorption efficiency [26]. To address this problem, a heterostructure was constructed by ZnO/CuO. CuO is a p–type metal oxide with a narrow band gap of 1.20 eV. This narrow band gap will accelerates the recombination of electron–hole [27]. By synthesizing a kind of ZnO/CuO p–n heterostructure nanocomposite, the separation efficiency of the electron–hole can be accelerated and the recombination of the electron–hole can be reduced. ZnO/CuO effectively compensates for the deficiencies of ZnO and CuO, and the cathodic current is obtained under visible light irradiation [28].

The Fe_3O_4@SiO_2@CdS and ZnO/CuO are used as photosensitive materials in this work. The Fe_3O_4@SiO_2@CdS–DNA_1–CEA aptamer–DNA_2–ZnO/CuO immune complex was easily formed in PBS buffer solution and modified to detect the cathodic current. Low concentration of CEA can lead to the dissociation of the immune complex, and the interference in the real sample can be effectively removed by magnetic separation. The Fe_3O_4@SiO_2@CdS–DNA_1 collected by magnetic separation was modified on the electrode to detect the anodic photocurrent. Therefore, it is possible to avoid false positive or false negative test results caused by oxidation or reduction of interfering substances [29]. This PEC immunosensor has the advantages of high speed, high efficiency, high sensitivity, good specificity, and stability [30]. The sensing platform constructed by this work can also be extended to detect other targets, which provides a new idea for the PEC sensing platform [31].

2. Experimental part

2.1. Reagents and apparatus

The ITO conductive glass was acquired from Zhuhai Kaivo Electronic Components Co. Ltd., China. Other details were shown in supplementary material.

2.2. Preparation of Fe_3O_4@SiO_2@CdS–DNA_1

Firstly, 1 mL of Fe_3O_4@SiO_2@CdS suspension and chitosan acetic acid solution (3 mL, 0.1 wt%) were mixed and reacted at 50 °C for 2 h. After washing with ultrapure water, it was dispersed into glutaraldehyde aqueous solution (3 mL, 5 wt%), then heated at 38 °C for 1 h, magnetic separation, NH_2–DNA_1 (1 mL, 100 nmol/L) was added and incubated at 2 °C for 12 h. Finally, monoethanolamine (MEA) was added to obtain Fe_3O_4@SiO_2@CdS–DNA_1 at 2 °C.

2.3. Preparation of DNA_2–ZnO/CuO

55 mg of ZnO/CuO was added to ethanol/water solution (25 mL,

$V_{ethanol}/V_{water}$ = 19/1). Then, 1 mL of APTES was added to the ZnO/CuO suspension, and the mixed suspension was heated at 70 °C for 1 h. After cooling, the suspension was centrifuged and washed 3 times with ethanol. It was redispersed in 5 mL of ultrapure waterto obtain amino–functionalized ZnO/CuO. It was stirred at room temperature for 12 h, then SH–DNA_2 (10 μL, 10 μmol/L) was added, stirred for 10 h, then centrifuged and washed 3 times with ultrapure water to obtain DNA_2–ZnO/CuO.

2.4. Preparation of Fe_3O_4@SiO_2@CdS–DNA_1–CEA aptamer–DNA_2–ZnO/CuO

The 1 mL (200 nmol/L) DNA_2–ZnO/CuO and 1 mL (200 nmol/L) CEA aptamer solution containing 20 mmol/L $MgCl_2$ was mixed to form a uniform solution. Then 1 mL (200 nmol/L) Fe_3O_4@SiO_2@CdS–DNA_1 containing 20 mmol/L $MgCl_2$, Fe_3O_4@SiO_2@CdS–DNA_1–CEA aptamer–DNA_2–ZnO/CuO composite were formed by partial hybridization reaction within 1 h at 37 °C, extracted and washed by external magnetic field and dispersed in 1 mL deionized water. Fe_3O_4@SiO_2@CdS–DNA_1–CEA aptamer–DNA_2–ZnO/CuO immune hybrid was obtained.

2.5. Fabrication of PEC immunosensor

The construction process of the PEC immunosensor was shown in Scheme 1. The ITO conductive glass electrode (0.8 × 2.0 cm^2) was successively cleaned with detergent, acetone, ethanol, and ultrapure water, and dried in a nitrogen atmosphere. The PEC immunosensor was fabricated on ITO electrode. Different concentration of CEA (1–10000 pg/mL) were incubated with Fe_3O_4@SiO_2@CdS–DNA_1–CEA aptamer–DNA_2–ZnO/CuO at 4 °C for 2 h. After magnetic separation, 20 μL of product containing separated Fe_3O_4@SiO_2@CdS–DNA_1 was modified on the ITO electrode and dried at 25 °C, and dried naturally at room temperature. Finally, the electrode was washed with PBS (pH = 7.4) and prepared for the PEC measurement.

2.6. PEC measurement

The photocurrent was measured on the PEC workstation (CHI 760E Chenhua Instrument Company, Shanghai, China). Other details were shown in supplementary material.

3. Results and discussion

3.1. Characterization of synthesized materials

In order to verify the success of ZnO/CuO preparation, the as–synthesized nanocomposites were characterized. Fig. 1A shows the X–ray diffraction (XRD) pattern of ZnO/CuO, in which the diffraction peaks at 31.8°, 34.4°, 26.3°, 47.5°, 56.6°, 62.9°, and 38.0° are attributed to (100), (001), (101), (102), (110), (103), and (112) crystal faces of ZnO (JCPDS 36–1541). The diffraction peaks at 35.5°, 38.7°, 38.9°,

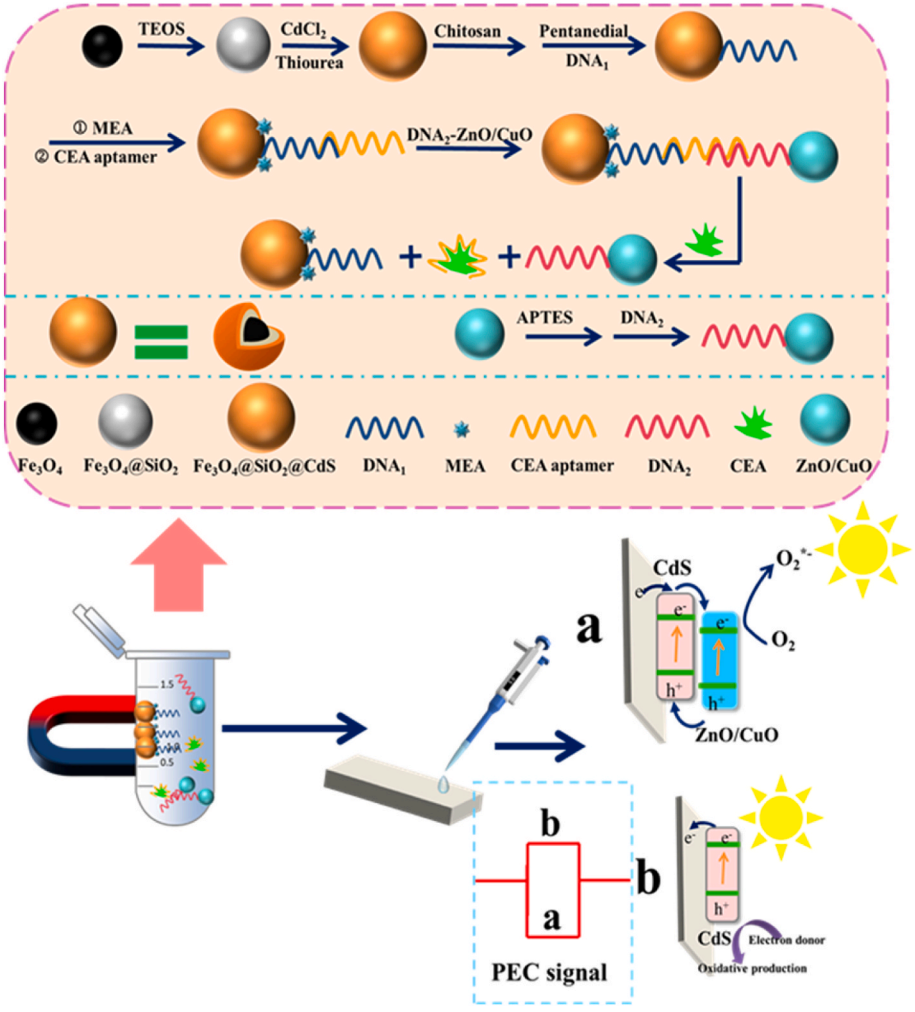

Scheme 1. Fabrication process of PEC immunosensor. Possible photogeneration electron transfer mechanisms for (a) Fe_3O_4@SiO_2@CdS–DNA_1–CEA–aptamer–DNA_2–ZnO/CuO and (b) Fe_3O_4@SiO_2@CdS–DNA_1.

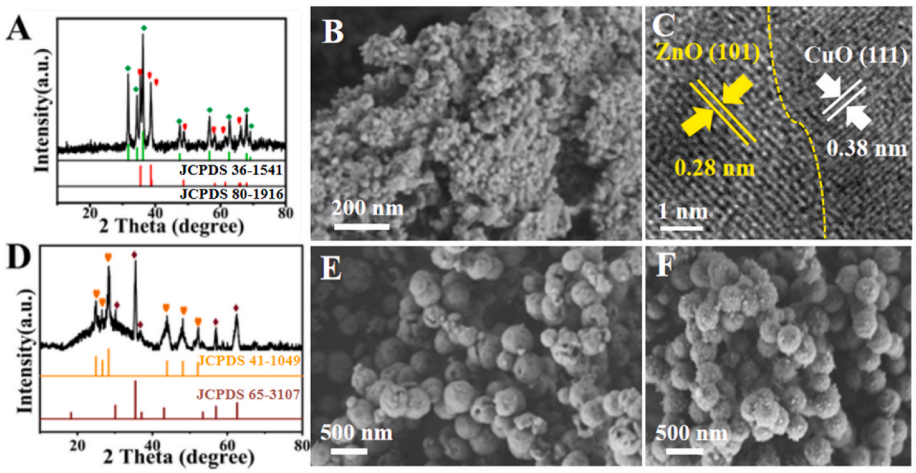

Fig. 1. (A) XRD pattern and (B) SEM image of ZnO/CuO, (C) HRTEM image of ZnO/CuO (D) XRD pattern of Fe_3O_4@SiO_2@CdS, (E) SEM image of Fe_3O_4@SiO_2, (F) SEM image of Fe_3O_4@SiO_2@CdS.

48.7°, 58.2°, 51.4°, 57.7°, 66.1°, and 68.0°can well correspond to the (−111), (111), (200), (−202),(202), (−113), (022), (−311), (022), and (220) crystal planes of CuO (JCPDS 80–1916). Fig. 1B shows the scanning electron microscope (SEM) image of ZnO/CuO, from which we can see that ZnO/CuO exhibited a sphere–like structure with a diameter of about 20 nm. Fig. 1C shows the high resolution transmission electron microscopy (HRTEM) image ZnO/CuO, it can be clearly observed the crystal boundary with the ZnO (101) of 0.28 nm and CuO (111) of 0.38 nm. In addition, XRD (Fig. 1D) and SEM (Figure S1, Fig. 1E and F) tests were performed on Fe_3O_4@SiO_2@CdS. The peaks at 18.3°, 30.1°, 35.4°, 37.1°, 43.1°, 53.5°, 56.9°, and 62.6°correspond to the peaks of Fe_3O_4 (JCPDS 65–3107). In particular, the characteristic diffraction peak at 17.28° can be attributed to the amorphous SiO_2 (JCPDS 29–0085). The peaks at 24.8°, 26.5°, 28.2°, 43.8°, and 52.8° correspond to the crystal plane of CdS (JCPDS 41–1049). In addition, the Fe_3O_4 and Fe_3O_4@SiO_2, and Fe_3O_4@SiO_2@CdS were characterized in the synthesis process. Figure S1, Fig. 1E and 1F are SEM images of Fe_3O_4 and Fe_3O_4@SiO_2, and Fe_3O_4@SiO_2@CdS, respectively. It is obvious in the image that a relatively smooth SiO_2 film is deposited to the surface of Fe_3O_4@SiO_2 compared to Fe_3O_4. Compared to Fe_3O_4@SiO_2, CdS particles were observed on the surface of Fe_3O_4@SiO_2@CdS. It is verified that the composite material is a gradually coated core–shell structure.

3.2. Possible mechanism of PEC immunoassay

The possible electron transfer mechanism of the proposed PEC immunosensor. In the absence of CEA, the sandwich immune complex Fe_3O_4@SiO_2@CdS–DNA_1–CEA aptamer–DNA_2–ZnO/CuO is formed in the solution and fixed on the photoelectrode, in which the ZnO/CuO in the immune complex plays a leading role. Under radiation by light, the majority of the electrons transfer from the CB of CdS to the CB of ZnO/CuO and then trapped by the electron acceptor in the solution, resulting in a cathodic current. When the CEA and the sandwich immune complex are fully reacted in the solution, the sandwich immune complex is dissociated due to the combination of CEA and the CEA aptamer. As the CEA concentration increases, Fe_3O_4@SiO_2@CdS gradually increases in the solution and plays a leading role. The magnetic products are collected and fixed on the electrode by magnetic separation, and the electrons are excited by light to transition from the VB to the CB of the CdS and transfer to the electrode direction, resulting in an anode photocurrent. During the detection process, it can be observed that the as–prepared sensor gradually changes the photocurrent from the cathode to the anode as the CEA concentration increases. This strategy of changing the direction of the signal during the detection process can achieve highly sensitive detection of CEA.

3.3. Characterization of the PEC immunosensor

By testing during the modification process, it can be proved that each step of the experiment was successfully completed. As shown in Fig. 2A, curve a indicates that the photocurrent value of Fe_3O_4@SiO_2@CdS is about 143.8 nA. The photocurrent value of Fe_3O_4@SiO_2@CdS–DNA_1 (curve b) decreases to 123.6 nA. This is due to the fact that the protein molecule is a biomolecule that acts as a barrier to electron transfer. When the photocurrent value of Fe_3O_4@SiO_2@CdS–DNA_1–CEA aptamer was further examined to be 73.4 nA (curve c), the photocurrent further decreased, but the direction was still positive. After the preparation of Fe_3O_4@SiO_2@CdS–DNA_1–CEA aptamer–DNA_2–ZnO/CuO, the photocurrent value (−75.5 nA, curve d) was detected, and it was found that the direction of the photocurrent changed. This indicates that each step in the sensor synthesis process was successful.

Moreover, electrochemical impedance spectroscopy (EIS) is used to prove the success of the electrode layer modification. The impedance was measured in the frequency range of 0.1 Hz–100000 Hz with an amplitude parameter of 5 mV and a bias voltage of 0 V. As shown in Fig. 2B, Fe_3O_4@SiO_2@CdS (curve a) has the smallest diameter, and the diameters of Fe_3O_4@SiO_2@CdS–DNA_1 (curve b), Fe_3O_4@SiO_2@CdS–DNA_1–CEA aptamer (curve c) and Fe_3O_4@SiO_2@CdS–DNA_1–CEA aptamer–DNA_2–ZnO/CuO (curve d) gradually increase, indicating that the gradual resistivity increases in turn, proving that each step is successfully prepared. This is due to the insulating effect of the protein molecules, which prevents the transfer of electrons.

3.4. PEC determination of CEA

The calibration curve of the sensor is detected and fitted under the most ooptimal conditions, and the result is shown in Fig. 3. There is an excellent linear relationship between the photocurrent and the logarithm of the CEA concentration in the range of 1–10000 pg/mL. The regression equation is $I = 34.68 \cdot \lg c$ (pg/mL) – 59.24, and the correlation coefficient is 0.9995. The detection limit (LOD, S/N = 3) of the sensor is about 0.34 pg/mL.

3.5. Reproducibility and specificity of the PEC immunosensor

In order to make this work more rigorous, the reproducibility, selectivity, and stability of the immunosensor were tested. In order to verify that the constructed PEC immunosensor has good reproducibility, we constructed five electrodes under the same conditions and tested the photocurrent (Fig. 4A). The relative standard deviation (RSD) of these five groups of immunosensors is less than 2.65 %, indicating that the

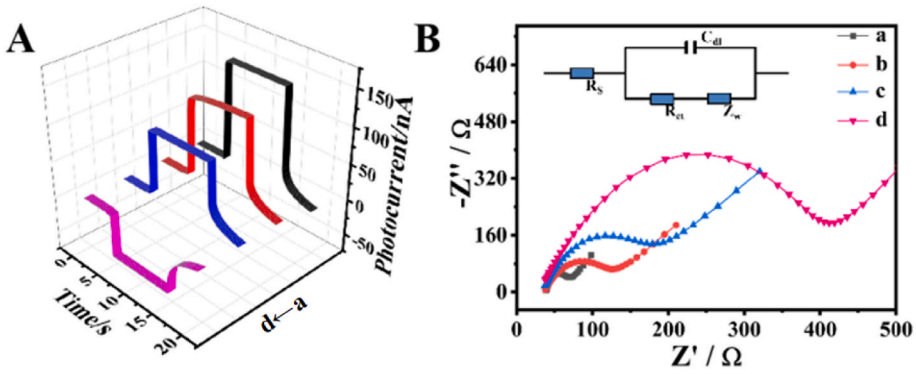

Fig. 2. (A) Photocurrent responses and (B) Nyquist diagrams of (a) the bare Fe_3O_4@SiO_2@CdS, (b) Fe_3O_4@SiO_2@CdS–DNA_1, (c) Fe_3O_4@SiO_2@CdS–DNA_1–CEA aptamer, (d) Fe_3O_4@SiO_2@CdS–DNA_1–CEA aptamer–DNA_2–ZnO/CuO. Inset of part B: the electrical equivalent circuit applied to fit the impedance spectra.

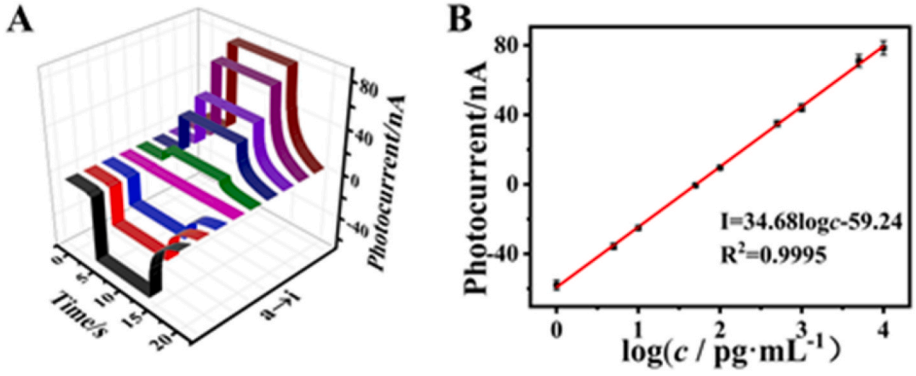

Fig. 3. (A) PEC immunosensor photocurrent response and (B) the corresponding calibration curve of the photocurrent measured in 0.1 mol/L PBS (pH = 7.0) containing CEA concentration at 1, 5 10, 50, 100, 500, 1000, 5000, 10000 pg/mL at a bias voltage of 0 V with chopped light irradiation.

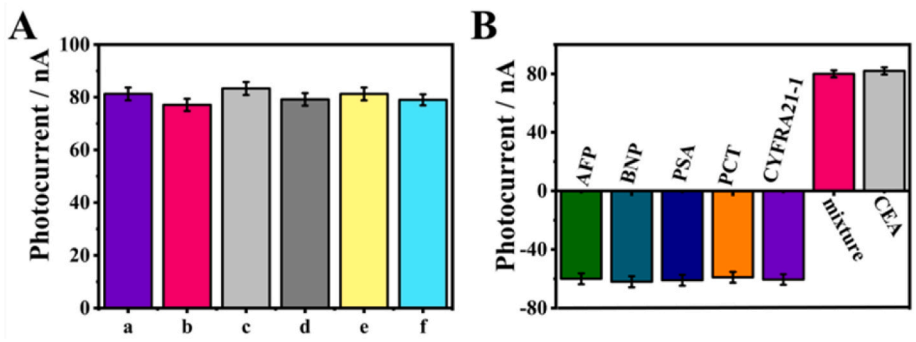

Fig. 4. (A) Stability test of the PEC immunosensor, (B) Selectivity of the PEC sensing platform for CEA detection CEA (10 ng/mL); interferent (100 ng/mL); the mixture containing CEA (10 ng/mL), and five interferents (the concentration of each interferent, 100 ng/mL). Error bars = SD (n = 3).

sensor can be easily repeated.

Specificity is a necessary property of the constructed PEC immunosensor. Here, we selected alpha–fetoprotein (AFP), brain natriuretic peptide (BNP), prostate–specific antigen (PSA), procalcitonin (PCT), and cytokeratin 19 fragment 21–1 (CYFRA21–1) as interfering antigens to determine the specificity of the proposed PEC immunosensor. The concentration of the interfering antigen was 100 ng/mL, while the concentration of CEA was 10 ng/mL. And the magnetic product obtained when only the interfering antigen was added to the immune sandwich complex was cathodic current. On the contrary, anodic photocurrent was detected when only CEA and the solution containing CEA and interference antigen were present. This shows that the sensor can realize the specific detection of CEA. This is because only CEA can cause the dissociation of the sandwich immune complex. This shows that the constructed PEC immunosensor has good specificity.

3.6. Real simple detection

In order to verify the feasibility of the proposed PEC immunosensor for the detection of CEA in complex serum samples, the standard addition method was used to detect CEA in the serum samples. The experimental results are shown in Table S1. The average recovery rate of this PEC immunosensor is in the range of 100.2–102.8 %, and the RSD is 1.23–2.84 %. Therefore, the PEC immunosensor platform has good accuracy in clinical diagnosis.

4. Conclusion

In this study, a polarity switching PEC immunosensor with good magnetic and optoelectronic properties was successfully prepared. Fe_3O_4@SiO_2@CdS was chosen as the substrate material, and ZnO/CuO was used as the signaling marker with excellent photocurrent response. The PEC immunosensor can achieve highly sensitive and selective detection of CEA with a detection range of 1–10000 pg/mL and a detection limit of 0.34 pg/mL. The magneto–optical nanostructures and photocurrent polarity–switching sensing platforms provide novel and unique inspirations for the detection of other disease markers or environmental pollutants.

CRediT authorship contribution statement

Xiang Ren: Methodology, Funding acquisition. **Man Wang:** Investigation. **Jinxiu Zhao:** Software, Methodology. **Jinhuan Zhang:** Methodology, Formal analysis. **Jingui Chen:** Writing – original draft, Methodology. **Faying Li:** Writing – review & editing, Funding acquisition. **Qin Wei:** Writing – review & editing, Funding acquisition. **Huangxian Ju:** Writing – review & editing.

Declaration of competing interest

The authors declare that they have no known competing financial interests or personal relationships that could have appeared to influence the work reported in this paper.

Data availability

Data will be made available on request.

Acknowledgments

This study was supported by the National Natural Science Foundation of China (No. 22204059, 22274062), the Natural Science Foundation of Shandong Province (No. ZR2021QB120), the Excellent Youth Innovation Team of Higher Education Institutions in Shandong Province (2023KJ317), the Yunnan Provincial Key Laboratory of Rural Energy Engineering (Yunnan Normal University) Open Fund (2022KF007). Shandong Medical and Health Science and Technology Project (No. 202326020474) and the Young Taishan Scholars Program of Shandong Province of China (No.tsqnz20231234).

Appendix A. Supplementary data

Supplementary data to this article can be found online at https://doi.org/10.1016/j.aca.2024.342703.

References

[1] S.A. Lasser, F.G. Ozbay Kurt, I. Arkhypov, J. Utikal, V. Umansky, Myeloid–derived suppressor cells in cancer and cancer therapy, Nat. Rev. Clin. Oncol. 21 (2) (2024) 147–164, https://doi.org/10.1038/s41571–023–00846–y.

[2] C. Zhao, C. Ma, M. Wang, W. Lai, C. Hong, Electrochemiluminescence enhancement and passivation mitigation in carbon nitride semiconductors via an integrated ternary heterostructure strategy, Small n/a (n/a) (2024) 2310476, https://doi.org/10.1002/smll.202310476.

[3] J. Chen, N. Song, N. Zhang, Z. Gao, D. Wu, H. M, X. Ren, Q. Wei, Smartphone–controlled portable photoelectrochemical immunosensor for point–of–care testing of carcinoembryonic antigen, Chem. Eng. J. 473 (2023), https://doi.org/10.1016/j.cej.2023.145276.

[4] T. Yasuda, Y.A. Wang, Gastric cancer immunosuppressive microenvironment heterogeneity: implications for therapy development, Trends in Cancer (2024), https://doi.org/10.1016/j.trecan.2024.03.008.

[5] V. Garg, A.M. Oza, Assessment of homologous recombination deficiency in ovarian cancer, Clin. Cancer Res. 29 (16) (2023) 2957–2960, https://doi.org/10.1158/1078–0432.ccr–23–0563.

[6] L. Li, Y. Bo, P. Miao, J. Chang, Y. Zhang, B. Ding, Y. Lv, X. Yang, J. Zhang, M. Yan, Self–powered photoelectrochemical immunosensing platform for sensitive CEA detection using dual–photoelectrode synergistic signal amplification, Biosens. Bioelectron. 250 (2024) 116075, https://doi.org/10.1016/j.bios.2024.116075.

[7] T. Nordström, M. Annerstedt, A. Glaessgen, S. Carlsson, M. Clements, A. Abbadi, H. Grönberg, F. Jäderling, M. Eklund, A. Discacciati, Repeated prostate cancer screening using prostate–specific antigen testing and magnetic resonance imaging: a secondary analysis of the STHLM3–MRI randomized clinical trial, JAMA Netw. Open 7 (2) (2024) e2354577, https://doi.org/10.1001/jamanetworkopen.2023.54577.

[8] A. Jing, Q. Xu, W. Feng, G. Liang, An electrochemical immunosensor for sensitive detection of the tumor marker carcinoembryonic antigen (CEA) based on three–dimensional porous nanoplatinum/graphene, Micromachines 11 (7) (2020), https://doi.org/10.3390/mi11070660.

[9] W. Luo, Z. Ye, P. Ma, Q. Wu, D. Song, Preparation of a disposable electrochemiluminescence sensor chip based on an MXene–loaded ruthenium luminescent agent and its application in the detection of carcinoembryonic antigens, The Analyst 147 (9) (2022) 1986–1994, https://doi.org/10.1039/d2an00450j.

[10] J. Chen, J. Zhao, J. Feng, D. Wu, H. Ma, X. Ren, Q. Wei, H. Ju, Photoelectrochemical immunosensor based on a 1D Fe_2O_3/3D Cd–$ZnIn_{2.2}S_y$ heterostructure as a sensing platform for ultrasensitive detection of neuron–specific enolase, Anal. Chem. 94 (50) (2022) 17396–17404, https://doi.org/10.1021/acs.analchem.2c02645.

[11] Q. Zhang, Y. Fu, K. Xiao, C. Du, X. Zhang, J. Chen, Sensitive dual–mode biosensors for CYFRA21–1 assay based on the dual–signaling electrochemical ratiometric strategy and "on–off–on" PEC method, Anal. Chem. 93 (17) (2021) 6801–6807, https://doi.org/10.1021/acs.analchem.1c00746.

[12] X. Ren, M. Wang, J. Chen, J. Zhao, H. Wang, D. Wu, R. Xu, Y. Zhang, H. Ju, Q. Wei, Sulfur defect–engineered Bi_2S_{3-x}/In_2S_{3-y} mediated signal enhancement of photoelectrochemical sensor for lead ions detection, Talanta 273 (2024), https://doi.org/10.1016/j.talanta.2024.125871.

[13] X. Ren, N. Song, J. Chen, M. Gao, H. Wang, Z.F. Gao, H. Ju, J. Zhao, Q. Wei, Oxygen vacancies–driven signal enhanced photoelectrochemical sensor for mercury ions detection, Talanta 272 (2024), https://doi.org/10.1016/j.talanta.2024.125780.

[14] Q. Liu, J. Kim, T. Cui, A highly sensitive photoelectrochemical sensor with polarity–switchable photocurrent for detection of trace hexavalent chromium, Sensor. Actuator. B Chem. 317 (2020) 128181, https://doi.org/10.1016/j.snb.2020.128181.

[15] J. Chen, J. Zhao, R. Feng, H. Ma, H. Wang, X. Ren, Q. Wei, H. Ju, Competitive photoelectrochemical aptamer sensor based on a Z–scheme Fe_2O_3/g–C_3N_4 heterojunction for sensitive detection of lead ions, J. Hazard Mater. 459 (2023), https://doi.org/10.1016/j.jhazmat.2023.132122.

[16] X. Ren, J. Chen, C. Wang, D. Wu, H. Ma, Q. Wei, H. Ju, Photoelectrochemical sensor with a Z–scheme Fe_2O_3/CdS heterostructure for sensitive detection of mercury ions, Anal. Chem. 95 (46) (2023) 16943–16949, https://doi.org/10.1021/acs.analchem.3c03088.

[17] J. Feng, N. Li, Y. Du, X. Ren, X. Wang, X. Liu, H. Ma, Q. Wei, Ultrasensitive double–channel microfluidic biosensor–based cathodic photo–electrochemical analysis via signal amplification of SOD–Au_PANI for cardiac troponin I detection, Anal. Chem. 93 (42) (2021) 14196–14203, https://doi.org/10.1021/acs.analchem.1c02922.

[18] Y. Zhang, T. Wu, D. Liu, R. Xu, H. Ma, Q. Wei, Y. Zhang, Photoelectrochemical immunosensor for the sensitive detection of neuron–specific enolase based on the effect of Z–scheme WO_3/$NiCo_2O_4$ nanoarrays p–n heterojunction, Biosens. Bioelectron. 213 (2022), https://doi.org/10.1016/j.bios.2022.114452.

[19] Y. Fu, Q. Yu, Q. Zhang, X. Zhang, C. Du, J. Chen, A photocurrent–polarity–switching biosensor for highly selective assay of mucin 1 based on target–induced hemin transfer from ZrO_2 hollow spheres to G–quadruplex nanowires, Biosens. Bioelectron. 192 (2021), https://doi.org/10.1016/j.bios.2021.113547.

[20] X. Niu, C. Lu, D. Su, F. Wang, W. Tan, F. Qu, Construction of a polarity–switchable photoelectrochemical biosensor for ultrasensitive detection of miRNA–141, Anal. Chem. 93 (40) (2021) 13727–13733, https://doi.org/10.1021/acs.analchem.1c03460.

[21] Y. Fu, K. Xiao, X. Zhang, C. Du, J. Chen, Peptide cleavage–mediated and environmentally friendly photocurrent polarity switching system for prostate–specific antigen assay, Anal. Chem. 93 (2) (2020) 1076–1083, https://doi.org/10.1021/acs.analchem.0c04086.

[22] J. Li, Y. Li, M. Han, X. Weng, Y. Li, Z. Lu, Q. Xu, H. Li, W. Wang, Superparamagnetic Fe_3O_4 nanoclusters embedded within porous TiO_2 shells for photoelectrochemical sensing, ACS Appl. Nano Mater. 3 (9) (2020) 9151–9157, https://doi.org/10.1021/acsanm.0c01797.

[23] Q. Zhang, H. Zheng, X. Zhang, C. Du, J. Chen, A universal "signal–on" and "photocurrent–polarity–switching" responsive photoelectrochemical aptasensing platform for dual–target assay based on two–hanging–arms tetrahedral DNAs, Sensor. Actuator. B Chem. 396 (2023) 134639, https://doi.org/10.1016/j.snb.2023.134639.

[24] N. Song, J. Chen, X. Ren, D. Wu, H. Ma, F. Li, H. Ju, Q. Wei, A signal amplifying photoelectrochemical immunosensor based on the synergism of Au@$CoFe_2O_4$ and CdS/$NiCo_2O_4$ for the sensitive detection of neuron–specific enolases, Sensor. Actuator. B Chem. 409 (2024), https://doi.org/10.1016/j.snb.2024.135593.

[25] W. Shi, D. Lu, L. Wang, F. Teng, J. Zhang, Core–shell structured Fe_3O_4@SiO_2@CdS nanoparticles with enhanced visible–light photocatalytic activities, RSC Adv. 5 (128) (2015) 106038–106043, https://doi.org/10.1039/c5ra22295h.

[26] G. Byzynski, C. Melo, D.P. Volanti, M.M. Ferrer, A.F. Gouveia, C. Ribeiro, J. Andrés, E. Longo, The interplay between morphology and photocatalytic activity

in ZnO and N–doped ZnO crystals, Mater. Des. 120 (2017) 363–375, https://doi.org/10.1016/j.matdes.2017.02.020.
[27] S. Konar, H. Kalita, N. Puvvada, S. Tantubay, M.K. Mahto, S. Biswas, A. Pathak, Shape–dependent catalytic activity of CuO nanostructures, J. Catal. 336 (2016) 11–22, https://doi.org/10.1016/j.jcat.2015.12.017.
[28] K. Zou, Y. Fu, R. Yang, X. Zhang, C. Du, J. Chen, CuO–ZnO heterojunction derived from Cu^{2+}–doped ZIF–8: a new photoelectric material for ultrasensitive PEC immunoassay of CA125 with near–zero background noise, Anal. Chim. Acta 1099 (2020) 75–84, https://doi.org/10.1016/j.aca.2019.11.054.
[29] M. Jiang, M. Wang, W. Lai, C. Zhao, C. Hong, X. Qiao, X. Song, Construction of an aptamer sensor for sensitive detection of AOH based on the enhancement of light/electric dual signaling response of Ru/Cu–THQ by Ag NCs, Chem. Eng. J. 485 (2024) 149911, https://doi.org/10.1016/j.cej.2024.149911.
[30] Y. Zhou, A. Abdurexit, R. Jamal, T. Abdiryim, X. Liu, F. Liu, F. Xu, Y. Zhang, Z. Wang, Highly sensitive electrochemical sensing of norfloxacin by molecularly imprinted composite hollow spheres, Biosens. Bioelectron. 251 (2024) 116119, https://doi.org/10.1016/j.bios.2024.116119.
[31] Q.u.A. Zahra, S. Ullah, F. Shahzad, B. Qiu, X. Fang, A. Ammar, Z. Luo, S. Abbas Zaidi, MXene–based aptasensors: advances, challenges, and prospects, Prog. Mater. Sci. 129 (2022) 100967, https://doi.org/10.1016/j.pmatsci.2022.100967.